MPC and DOB-based Robust Optimal Control of a New Quadrotor Manipulation System

Ahmed Khalifa[1], Mohamed Fanni[2] and Toru Namerikawa[3]

Abstract— This paper introduces motion control scheme of a new aerial manipulation system that consists of 2-link manipulator attached to the bottom of a quadrotor. This new system presents a solution for the limitations found in the current quadrotor manipulation systems. This new system are very attractive for a wide range of applications due to their unique features. However, control of such system is quite challenging because it is naturally unstable, has strong nonlinearities and couplings, are very susceptible to parameters variations due to carrying a payload besides the external disturbances like wind, and has actuator limitations. A robust optimal linear control scheme is proposed to address these issues. The proposed control scheme is based on a hybrid linear Model Predictive Control (MPC) and linear Disturbance Observer (DOb) techniques. The motivation for using DOb, apart from its property of providing robustness to the scheme in front of a significant class of nonlinearities/uncertainties, by estimating the nonlinear terms and external disturbances, allowing one to solve the model predictive control optimization problem relying on a set of linearized decoupled SISO systems which are not affected by nonlinear/uncertain terms. As a result, a standard MPC can be used and the resulting control scheme is characterized by a low computational load with respect to conventional nonlinear robust solutions. Stability analysis of the proposed control system is implemented. The controller is tested to achieve tracking of a point-to-point task space and trajectory quadrotor/joint space control under the effect of picking/placing a payload, changing the operating region, and measurement noise. System simulation is implemented in MAT-LAB/SIMULINK environment with real system parameters, to better emulate a realistic set up. Simulation results show the feasibility and effectiveness of the proposed control technique.

I. INTRODUCTION

Quadrotor is one of the Unmanned Aerial Vehicles (UAVs) which offer possibilities of speed and access to regions that are otherwise inaccessible to ground robotic vehicles. Quadrotor vehicles possess certain essential characteristics, such as small size and cost, Vertical Take Off and Landing (VTOL), and slow precise movements, which highlight their potential for use in vital applications [1]. Due to their superior mobility, much interest is given to utilize them for mobile manipulation such as inspection of hard-to-reach structures or transportation in remote areas. Several researches has been conducted in the area of aerial manipulation [2]–[9].

[1,2]Ahmed Khalifa and Mohamed Fanni are with the Department of Mechatronics and Robotics Engineering, Egypt-Japan University of Science and Technology, Alexandria, Egypt `ahmed.khalifa@ejust.edu.eg`
[2]Mohamed Fanni is on leave from Department of Production Engineering and Mechanical Design, Mansoura University, Mansoura, Egypt `mohamed.fanni@ejust.edu.eg`
[3]Toru Namerikawa is with the Department of System Design Engineering, Keio University, Yokohama, Japan `namerikawa@sd.keio.ac.jp`

However, the previous introduced systems in the literature that uses a gripper suffers from the limited allowable DOF of the end-effector. The other systems have a manipulator with either two DOF but in certain topology that disables the end-effector to track arbitrary 6-DOF trajectory, or more than two DOF which decreases greatly the possible payload carried by the system. Moreover, the control schemes that were presented in the literature for such robots are based on nonlinear controllers which are very complicated and have very high computational cost.

In [10], we propose a new aerial manipulation system that consists of a 2-link manipulator attached to the bottom of a quadrotor. This new system presents a solution for the limitations found in the current quadrotor manipulation systems. Firstly, our proposed aerial manipulator has the capability of manipulating the objects with arbitrary location and orientation because it posses 6-DOF. Secondly, it is based on a minimum manipulator weight for aerial manipulation (2-DOF manipulator). Thirdly, the manipulator provides sufficient and controlled distance between quadrotor and object location. In [11], the dynamic model of this system is derived taking into account the effect of adding/releasing a payload to the manipulator.

There are several issues when working with the aerial manipulation systems. The first one is achieving the position holding. In order to achieve this task, a robust control must be implemented such that it can reject uncertainties and disturbances in the system such as wind, payload changes, operation region changes, and measurement noise. The second issue with this system is the limitations of the actuators (thrusters and manipulator motors) which may degrade the performance if it is not considered during controller design. The third issue is the speed of the controller response which must be fast enough to be suitable with the high speed dynamics of the flying robot [12], so there is a need to design a low computational and fast response control algorithm.

To overcome the problem of robustness against nonlinearities, disturbances, uncertainties, measurements noise, and changes of the operating regions, we propose DOb based control technique to achieve the required robustness. The DOb estimate the nonlinear terms and uncertainties then compensates them such that the robotic system acts like a multi-SISO linear systems.

Disturbance Observer (DOb)-based controller is one of the most popular methods in the field of robust motion control due to its simplicity and computational efficiency. The authors in [13], [14] present the principles of DOb-based control system. In DOb-based robust motion control systems,

internal and external disturbances are observed by DOb, and the robustness is simply achieved by feeding-back the estimated disturbances in an inner-loop. Another controller is designed in an outer loop so that the performance goals are achieved without considering internal and external disturbances. In [15]–[18], DOb-based control technique has been applied to robotic systems and showed efficient performance. The stability analysis of DOb is investigated in [19], [20], which show that the system stability is guaranteed with the DOb-based control.

Therefore, it is possible to rely on the standard linear MPC methodology to design the controller of the outer loop such that the system performance can be adjusted to achieve desired tracking accuracy and speed, as well as actuators constraints with low computational load.

Model Predictive Control can represent an appropriate choice to solve this kind of issues partly, providing an optimal control strategy in case of complex constrained dynamical systems [21]–[24]. Its application to robotic systems in a true industrial environment, in which disturbances affect the robotic system and the model of the robot is inevitably inaccurate, is still limited. This is due to the high nonlinearity and uncertainties of dynamics in the robotics system. In [25], [26], a nonlinear MPC is utilized to solve the problem of the control of highly nonlinear systems. In [27], robust MPC control design based on feedback linearization and sliding mode control is utilized to achieve trajectory tracking of robotic manipulator. In [28], nonlinear MPC with nonlinear DOb is used to control a robotic system. However, the nonlinear control methods make the MPC to be more complex and has high computational cost which is not suitable to our robotic system.

This paper is organized as follows: In section II, the considered robotic system is described, and kinematic and dynamic analysis are reviewed. The control problem to solve is formulated and the DOb and MPC approaches are described in section III. In section IV, simulation results using MATLAB/SIMULINK are presented. Finally, the main contributions are concluded in section V.

II. DESCRIPTION AND MATHEMATICAL MODELING

3D CAD model of the proposed system is shown in Fig. 1. The system consists mainly of two parts; the quadrotor and the manipulator. Fig. 2 presents a sketch of the proposed system with the relevant frames which indicates the unique topology that permits the end-effector to achieve arbitrary pose. The frames satisfy the Denavit-Hartenberg (DH) convention [29]. The manipulator has two revolute joints. The axis of the first revolute joint (z_0), that is fixed to the quadrotor, is parallel to the body x-axis of the quadrotor (see Fig. 2). The axis of the second joint (z_1) is perpendicular to the axis of the first joint and will be parallel to the body y-axis of quadrotor at home (extended) configuration. Thus, the pitching and rolling rotation of the end-effector is now possible independently from the horizontal motion of the quadrotor. Hence, with this new system, the capability of
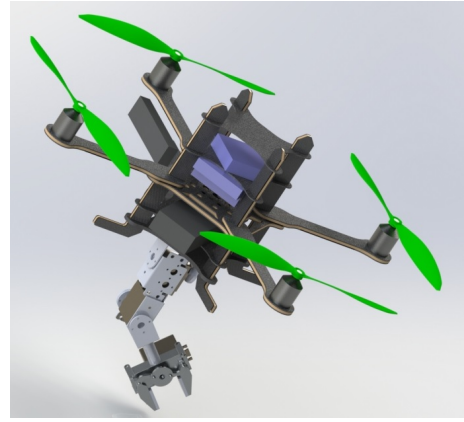

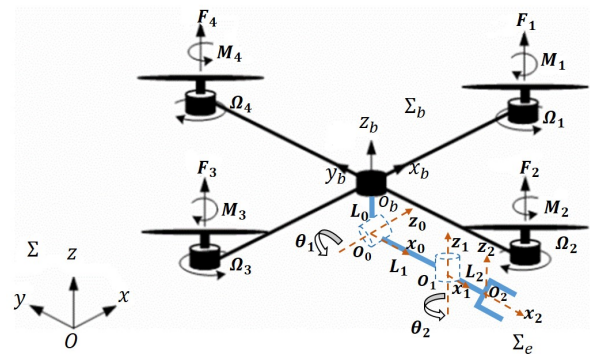Fig. 1: 3D CAD model of the New Quadrotor Manipulation System

Fig. 2: Schematic of Quadrotor Manipulation System with relevant frames

manipulating objects with arbitrary location and orientation is achieved. By this non-redundant system, the end-effector can achieve 6-DOF motion with minimum number of actuators/links which is an important factor in flight. The proposed system is distinguished from all other previous systems in the literature by having maximum mobility with minimum weight. The quadrotor components are selected such that it can carry a payload equals $500g$ (larger than the total arm weight and the maximum payload). Asctec pelican quadrotor [30] is used as the quadrotor platform. The maximum thrust force for each rotor is $6N$ as obtained from an identification process.

The arm components are designed, selected, purchased and assembled such that the total weight of the arm is $200g$, has maximum reach in the range between $22cm$ to $25cm$, and can carry a payload of $200g$. Three DC motors, (HS-422 (Max torque = $0.4N.m$) for gripper, HS-5485HB (Max torque = $0.7N.m$) for joint 1, and HS-422 (Max torque = $0.4N.m$) for joint 2), are used.

Each rotor j has angular velocity Ω_j and it produces thrust force F_j and drag moment M_j which are given by:

$$F_j = K_{f_j}\Omega_j^2 \tag{1}$$

$$M_j = K_{m_j}\Omega_j^2 \tag{2}$$

where K_{f_j} and K_{m_j} are the thrust and drag coefficients.

Let Σ_b, O_b- x_b y_b z_b, denotes the vehicle body-fixed reference frame with origin at the quadrotor center of mass, see Fig. 2. Its position with respect to the world-fixed inertial reference frame, Σ, O- x y z, is given by the $(3x1)$ vector $p_b = [x, y, z]^T$, while its orientation is given by the rotation matrix R_b:

$$R_b(\Phi_b) = \begin{bmatrix} C(\psi)C(\theta) & S(\psi)S(\theta)C(\psi) - S(\psi)C(\phi) & S(\psi)S(\phi) + C(\psi)S(\theta)C(\phi) \\ S(\psi)C(\theta) & C(\psi)C(\phi) + S(\psi)S(\theta)S(\phi) & S(\psi)S(\theta)C(\phi) - C(\psi)S(\phi) \\ -S(\theta) & C(\theta)S(\phi) & C(\theta)C(\phi) \end{bmatrix}, \tag{3}$$

where $\Phi_b=[\psi, \theta, \phi]^T$ is the triple ZYX yaw-pitch-roll angles. Note that $C(.)$ and $S(.)$ are short notations for $cos(.)$ and $sin(.)$. Let us consider the frame Σ_e, O_2- x_2 y_2 z_2, attached to the end-effector of the manipulator, see Fig. 2. Thus, the position of Σ_e with respect to Σ is given by

$$p_e = p_b + R_b p_{eb}^b, \tag{4}$$

where the vector p_{eb}^b describes the position of Σ_e with respect to Σ_b expressed in Σ_b. The orientation of Σ_e can be defined by the rotation matrix

$$R_e = R_b R_e^b, \tag{5}$$

where R_e^b describes the orientation of Σ_e w.r.t Σ_b.

The equations of motion of the proposed robot have been derived in details in [10]. Applying Newton Euler algorithm [31] to the manipulator considering that the link (with length L_0) that is fixed to the quadrotor is the base link, one can get the equations of motion of the manipulator as well as the interaction forces and moments between the manipulator and the quadrotor. The effect of adding a payload to the manipulator will appear in the parameters of its end link, link 2, (e.g. mass, center of gravity, and inertia matrix). The Newton Euler method are used to find the equations of motion of the quadrotor after adding the forces/moments from the manipulator.

The dynamical model of the quadrotor-manipulator system can be written as follows:

$$M(q)\ddot{q} + C(q, \dot{q})\dot{q} + G(q) + d_{ex} = \tau; \qquad \tau = Bu \tag{6}$$

where $q = [x, y, z, \psi, \theta, \phi, \theta_1, \theta_2]^T$ is $(8x1)$ vector of the generalized coordinates, M represents the symmetric and positive definite inertia matrix of the combined system, C is the matrix of Coriolis and centrifugal terms, G is the vector of gravity terms, d_{ex} is $(8x1)$ vector of the external disturbances, τ is $(8x1)$ vector of the generalized input torques/forces, $u = [F_1, F_2, F_3, F_4, \tau_{m_1}, \tau_{m_2}]^T$ is vector of the actuator inputs, $B = HN$ is the input matrix which is used to generate the body forces and moments from the actuator inputs. N is given by:
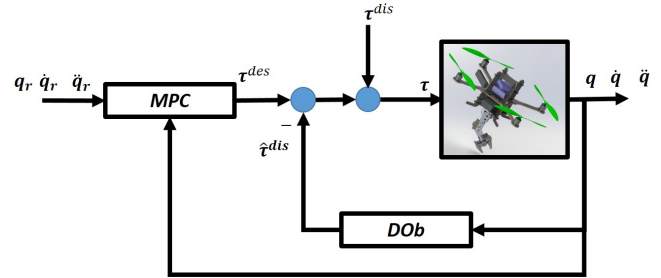

Fig. 3: Functional block diagram of the proposed control system

$$N = \begin{bmatrix} 0 & 0 & 0 & 0 & 0 & 0 \\ 0 & 0 & 0 & 0 & 0 & 0 \\ 1 & 1 & 1 & 1 & 0 & 0 \\ \gamma_1 & -\gamma_2 & \gamma_3 & -\gamma_4 & 0 & 0 \\ -d & 0 & d & 0 & 0 & 0 \\ 0 & -d & 0 & d & 0 & 0 \\ 0 & 0 & 0 & 0 & 1 & 0 \\ 0 & 0 & 0 & 0 & 0 & 1 \end{bmatrix} \tag{7}$$

where $\gamma_j = K_{m_j}/K_{f_j}$, and H is $(8x8)$ matrix that transforms body input forces to be expressed in Σ and is given by:

$$H = \begin{bmatrix} R_b & O_3 & O_2 \\ O_3 & T_b^T R_b & O_2 \\ O_{2x3} & O_{2x3} & I_2 \end{bmatrix} \tag{8}$$

III. CONTROLLER DESIGN

This section presents the proposed motion control strategy and DOb based control. Fig. 3 presents the functional block diagram of the proposed control system. In this control strategy, the system nonlinearities, uncertainties, external disturbances, τ^{dis}, are treated as disturbances which will be estimated, $\hat{\tau}^{dis}$, and canceled by the DOb in the inner loop. The system can be now considered as linear SISO plants and thus the MPC is used in the external loop to achieved the objective response for the system by producing τ^{des}.

A. Disturbance Observer Loop

A block diagram of the DOb inner loop is shown in Fig. 4.

In this figure, $M_n \in R^{8x8}$ is the system nominal inertia matrix, τ and τ^{des} are the robot and desired inputs, respectively, $P = Diag([g_1, ..., g_i, ..., g_8])$ with g_i

is the bandwidth of the ith variable of q, $Q(s) = Diag([\frac{g_1}{s+g_1}, ..., \frac{g_i}{s+g_i}, ..., \frac{g_8}{s+g_8}]) \in R^{8x8}$ is the matrix of the low pass filter of DOb. It is a well known fact that a DOb requires precise velocity measurement. Therefore, the velocity is estimated by using a low pass filter, $Q_v(s) = Diag([\frac{g_{v_1}}{s+g_{v_1}}, ..., \frac{g_{v_i}}{s+g_{v_i}}, ..., \frac{g_{v_8}}{s+g_{v_8}}]) \in R^{8x8}$, and with cut-off frequency of $P_v = Diag([g_{v_1}, ..., g_{v_i}, ..., g_{v_8}])$ (i.e. precise velocity measurement is achieved in a predetermined bandwidth). τ^{dis} represents the system disturbances including the Coriolis, centrifugal and gravitational terms, and $\hat{\tau}^{dis}$ represents the system estimated disturbances. The disturbance observer regards the difference between the actual input torque and output of the inverse of nominal model as an equivalent disturbance applied to the nominal model. This equivalent disturbance is fed back through low pass filter to cancel the actual disturbance. The roles of low pass filter are to diminish the high frequency noise in measured signal and to make the inverse of nominal system realizable. In this way, every disturbance acting on plant is dynamically canceled by feed forward compensation of filtered equivalent disturbance for designed frequency range. If we apply the concept of disturbance observer to the proposed system, the independent coordinate control is possible without considering coupling effect of other coordinates. The coupling terms such as centripetal and Coriolis and gravity terms are considered as disturbance and compensated by feed forward estimated disturbance torque.

The system disturbance τ^{dis} can be assumed as:

$$\tau^{dis} = (M(q) - M_n)\ddot{q} + \tau^d;$$
$$\tau^d = C(q,\dot{q})\dot{q} + G(q) + d_{ex} \tag{9}$$

Substituting from (9), then (6) can be rewritten as:

$$M_n\ddot{q} + \tau^{dis} = \tau \tag{10}$$

Now if the disturbance observer performs optimally, that is $\hat{\tau}^{dis} = \tau^{dis}$, the dynamics from the DOb loop input τ^{des} to the output of the robot manipulator is given by:

$$M_n\ddot{q} = \tau^{des} \tag{11}$$

Since M_n is a diagonal matrix, the system can be treated as multi-decoupled linear SISO systems as following:

$$M_{n_{ii}}\ddot{q}_i = \tau_i^{des}, \tag{12}$$

or simply in the acceleration space as:

$$\ddot{q}_i = \ddot{q}_i^{des} \tag{13}$$

The control input, τ, in Fig. 4 can be calculated as:

$$\tau = \frac{1}{(1-Q(s))}[M_n\ddot{q}^{des} - Q(s)M_n\ddot{q}]$$
$$= M_n\ddot{q}^{des} + M_nPe_v; \quad e_v = \dot{q}^{des} - \dot{q} \tag{14}$$

This control law leads to the following error dynamics:

$$M(q)\dot{e}_v + C(q,\dot{q})e_v + K_ve_v = \delta;$$
$$K_v = PM_n \tag{15}$$

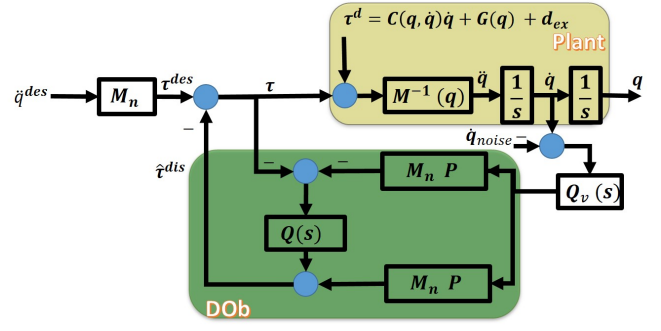Fig. 4: Block diagram of internal loop (DOb)

where

$$\delta = \Delta M(q)\ddot{q}^{des} + C(q,\dot{q})\dot{q}^{des} + G(q) + d_{ex};$$
$$\Delta M(q) = M(q) - M_n, \tag{16}$$

Equation (15) represents the error dynamics of DOb-based robust control of the quadrotor manipulation system.

To study the inner loop stability, assume the following Lyapunov function:

$$V = \frac{1}{2}e_v^T M(q)e_v + \frac{1}{2}\delta^T\delta \tag{17}$$

The time derivative of this function is:

$$\dot{V} = e_v^T M(q)\dot{e}_v + \frac{1}{2}e_v^T \dot{M}(q)e_v + \delta^T\dot{\delta} \tag{18}$$

Substituting from (15),

$$\dot{V} = e_v^T\delta - e_v^T K_ve_v + \frac{1}{2}e_v^T(\dot{M}(q) - 2C(q,\dot{q}))e_v + \delta^T\dot{\delta} \tag{19}$$

The dynamic equation of motion (6) posses several well known properties [29], [32]. These properties will be used to complete the stability analysis and they are stated as follows:

$$\lambda_{min}\|\nu\|^2 \le \nu^T M(q)\nu \le \lambda_{max}\|\nu\|^2 \tag{20}$$

$$\nu^T(\dot{M}(q) - 2C(q,\dot{q}))\nu = 0 \tag{21}$$

where $\dot{M}(q) - 2C(q,\dot{q})$ is a skew-symmetric matrix, $\nu \in R^8$ represents a 8-dimensional vector, and λ_{min} and λ_{max} are positive real constants.

Substituting from (21) into (19) with the assumption that δ changes very slow (i.e. $\dot{\delta} = 0$):

$$\dot{V} = e_v^T\delta - e_v^T K_ve_v \tag{22}$$

From the robot dynamic properties:

$$\dot{V} \le -\gamma V + \sqrt{\frac{2V}{\lambda_{min}}}|\delta|;$$
$$\gamma = \frac{2K_v}{\lambda_{max}} \tag{23}$$

Thus, the time derivative of the Lyapunov function is smaller than zero and the convergence rate increases proportionally with K_v. However, by inspecting the inner loop, one can find that there is a practical constraint on the choice of K_v due

to the usage of the velocity filter. The characteristic equation of the inner loop can be driven as:

$$P_{c_i} = s^2 + g_{v_i}s + \alpha_i g_i g_{v_i}, \qquad (24)$$

where, $\alpha_i = \frac{M_{n_{ii}}}{M_{ii}}$ The damping coefficient of this equation is $0.5\sqrt{\frac{g_i g_{v_i}}{\alpha g_i}}$, which should larger than or equal 0.707 to improve the robustness against both disturbances and noise. Thus, the following inequality should be hold:

$$\alpha g_i \le \frac{g_{v_i}}{2}, \qquad (25)$$

Rewrite (25) with respect to K_v,

$$\frac{K_{v_i}}{M_{ii}} \le \frac{g_{v_i}}{2}, \qquad (26)$$

To sum up, (23) shows that the stability and robustness of the control system is improved by increasing K_v (i.e. by increasing M_n and P) but without violating the robustness constraint in (26).

B. Linear Model Predictive Control

By virtue of the rejection of the nonlinearities, disturbances, uncertainties, and noise through the use of DOb internal loop, the MPC controller have not to consider uncertainties and can designed based on the nominal 8 SISO decoupled models of the system with satisfying the actuators constraints, $u_{min} \le u \le u_{max}$.

The SISO model of the system is given by:

$$\dot{x}_p(t) = A_p x_p(t) + B_p u_{mpc}(t)$$
$$q_i(t) = C_p x_p(t) \qquad (27)$$

where, $A_p = \begin{bmatrix} 0 & 0 \\ 1 & 0 \end{bmatrix}$, $B_p = \begin{bmatrix} 1 \\ 0 \end{bmatrix}$, $C_p = \begin{bmatrix} 0 & 1 \end{bmatrix}$, and $u_{mpc}(t)$ is the output of the MPC which will be $\ddot{q}^{des}$. The general design philosophy of model predictive control is to compute a trajectory of a future manipulated variable $u_{mpc}(t)$ to optimize the future behavior of the plant output $q_i(t)$. The optimization is performed within a limited time window starts by t_i with length T_p. To achieve offset free MPC, it will be designed based on an augmented model of the plant which is given as following:

$$\dot{x}(t) = Ax(t) + B\dot{u}_{mpc}(t)$$
$$q_i(t) = Cx(t) \qquad (28)$$

where, $x(t) = \begin{bmatrix} \dot{x}_p(t) \\ q_i(t) \end{bmatrix}$ $A = \begin{bmatrix} A_p & O_{2\times1} \\ C_p & 1 \end{bmatrix}$, $B = \begin{bmatrix} B_p \\ 0 \end{bmatrix}$, $C = \begin{bmatrix} O_{1\times2} & 1 \end{bmatrix}$,

The MPC design is based on the solution of the so-called Finite Horizon Optimal Control Problem which consists of minimizing a suitably defined cost function with respect to the control sequence. The cost function is given as:

$$J = \int_0^{T_p} (q_r(t_i) - q(t_i + \iota|t_i))^T Q_{mpc}(q_r(t_i) - q(t_i + \iota|t_i))$$
$$+ \dot{u}_{mpc}^T(\iota) R_{mpc} \dot{u}_{mpc}(\iota) d\iota \qquad (29)$$

where Q_{mpc} and R_{mpc} are weighting matrices that must be positive definite to ensure the stability of the outer loop [22].

Obtaining the plant response model is a key part of the implementation of an MPC controller. In our design, the controller models the system response using a generic function series approximation technique based on Laguerre polynomials [33] with parameters; a which is the scaling factor and b is the number of terms of Laguerre polynomials. This approach provides a simple and efficient method to mathematically model the process response with a minimum of a priori information. By applying the principle of receding horizon control (i.e., the control action will use only the derivative of the future control signal at $\iota = 0$), one can get the derivative of the optimal control for the unconstrained problem.

The next step is to formulate the constraints as part of design requirements, then translate them into linear inequalities, and relate them to the original model predictive control problem. Since the predictive control problem is formulated and solved in the framework of receding horizon control, the constraints are taken into consideration frame-by-frame for each moving horizon window. A simple algorithm, called Hildreth's quadratic programming procedure [34], was proposed for solving this problem. If there are many constraints, the computational load is quite large. Thus, in this method, the constraints that are not active is identified systematically, so they can then be eliminated in the solution. This method will lead to very simple programming procedures for finding real time optimal solutions of constrained minimization problem.

To design the MPC with prescribed degree of stability and closed loop performance can be performed as following [24], [35]: If the matrix A contains unstable poles due to the plant itself or the embedded integrator, then it better to move poles of the system to the stable region. This is can be achieved by modifying this matrix to be $(A - \varrho I)$ and Q_{mpc} to $(Q_{mpc} + 2\varrho P_{mpc})$, where P_{mpc} is the solution of the Riccati equation. The selection of ϱ is to make sure that the design model with $(A - \varrho I)$ is stable with all eigen values on the left-half of the complex plane. In order to specify the closed-loop response speed, a new tuning parameter is used β. During solution of Riccati equation the A matrix is modified to $(A + \beta I)$ and Q_{mpc} to $(Q_{mpc} + 2(\varrho + \beta)P_{mpc})$.

Fig. 5 shows the complete hybrid block diagram of the proposed control system. Since the vehicle (quadrotor) is an under-actuated system, i.e., only 4 independent control inputs are available against the 6 DOF, the position and the yaw angle are usually the controlled variables, while pitch and roll angles are used as intermediate control inputs for horizontal positions control. Therefore, the proposed control system consists from two DOb-based controllers by dividing q in to two parts; one for $\zeta = [x, y, z, \psi, \theta_1, \theta_2]$ (with MPC_ζ, M_{n_ζ}, P_ζ, Q_ζ) and the other for $\sigma_b = [\theta, \phi]$ (with MPC_σ, M_{n_σ}, P_σ, Q_σ). The desired trajectories for the end-effector's position and orientation ($p_{e,d}$ and $\Phi_{e,d}$) are fed to the inverse kinematics algorithm together with $\sigma_{b,r}(t)$ from a simplified version of the nonholonomic constraints
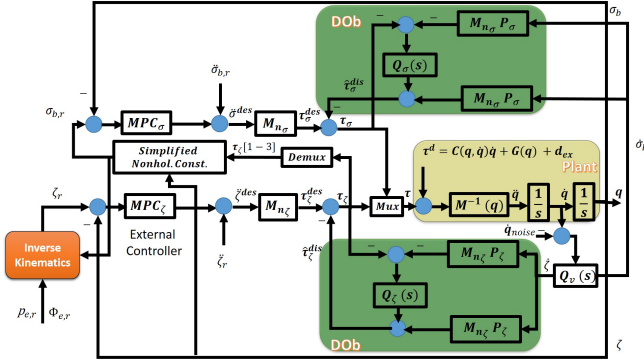
Fig. 5: Block diagram of the detailed control system for the quadrotor manipulation system

TABLE I: System Parameters

Par.	Value	Unit	Par.	Value	Unit
m	1	kg	L_2	$85x10^{-3}$	m
d	$223.5X10^{-3}$	m	m_0	$30x10^{-3}$	kg
I_x	$13.215X10^{-3}$	$N.m.s^2$	m_1	$55x10^{-3}$	kg
I_y	$12.522X10^{-3}$	$N.m.s^2$	m_2	$112x10^{-3}$	kg
I_z	$23.527X10^{-3}$	$N.m.s^2$	I_r	$33.216X10^{-6}$	$N.m.s^2$
L_0	$30x10^{-3}$	m	L_1	$70x10^{-3}$	m
K_{F_1}	$1.667x10^{-5}$	$kg.m.rad^{-2}$	K_{F_2}	$1.285x10^{-5}$	$kg.m.rad^{-2}$
K_{F_3}	$1.711x10^{-5}$	$kg.m.rad^{-2}$	K_{F_4}	$1.556x10^{-5}$	$kg.m.rad^{-2}$
K_{M_1}	$3.965x10^{-7}$	$kg.m^2.rad^{-2}$	K_{M_2}	$2.847x10^{-7}$	$kg.m^2.rad^{-2}$
K_{M_3}	$4.404x10^{-7}$	$kg.m^2.rad^{-2}$	K_{M_4}	$3.170x10^{-7}$	$kg.m^2.rad^{-2}$

TABLE II: Controller parameters

$Parameter$	$Value$
M_{n_ζ}	$Diag\{1.2, 1.2, 2, 0.5, 0.005, 0.005\}$
M_{n_σ}	$Diag\{0.5, 0.5\}$
Q_{mpc_ζ}	$C^T C$
Q_{mpc_σ}	$C^T C$
R_{mpc_ζ}	I_6
R_{mpc_σ}	I_2
ϱ_{mpc_ζ}	10
ϱ_{mpc_σ}	15
β_{mpc_ζ}	5
β_{mpc_σ}	10
u_{max}	$[6, 6, 6, 6, 0.7, 0.4]$
u_{min}	$[0, 0, 0, 0, -0.7, -0.4]$
P_ζ	$Diag\{2.4, 2.4, 14.5, 0.6950, 19.5, 4.5\}$
P_σ	$Diag\{1.3, 0.76\}$
g_{v_i}	100
a	0.6
b	6
T_p	70

such that the desired vehicle/joint space trajectories $\zeta_r(t)$ are obtained. After that, the controller block receives the desired trajectories and the feedback signals from the system and provides the control signal, τ. The desired values $\sigma_{b,r}$ for the intermediate controller are obtained from the output of position controller, τ_ζ, through the following simplified nonholonomic constraints relation:

$$\sigma_{b,r} = \frac{1}{\tau_\zeta(3)} \begin{bmatrix} C(\psi) & S(\psi) \\ S(\psi) & -C(\psi) \end{bmatrix} \begin{bmatrix} \tau_\zeta(1) \\ \tau_\zeta(2) \end{bmatrix} \qquad (30)$$

However, the response of the σ controller must be much faster than that of the quadrotor position controller such that it can track the changes in the position controller. This can be achieved by the tuning parameters of both DOb and MPC, as it is explained previously.

The output of two controllers, τ_ζ and τ_σ, are mixed to generate the final control vector τ which is then converted to the forces/torques applied to quadrotor/manipulator through the following relation:

$$u = B^{-1} \begin{bmatrix} \tau_\zeta(1:4) \\ \tau_\sigma \\ \tau_\zeta(5:6) \end{bmatrix} \qquad (31)$$

IV. SIMULATION RESULTS

In this section the previously proposed control strategy is applied in simulation MATLAB/SIMULINK program to the model of the considered aerial manipulation robot. Note that the model has been identified on the basis of real data through experimental tests, and a normally distributed measurement noise, with mean of 10^{-3} and standard deviation of $5x10^{-3}$, has been added to the measured signals. As a result, the simulation environment is quite realistic. The identified parameters are given in Table I.

To achieve task space control, the desired values of end-effector position and orientation, $p_{e,r}$ and $\Phi_{e,r}$, (Multi operational regions and point-to-point control) are used to generate the desired trajectories for ζ using the inverse kinematics and then applied to the algorithm for generating the desired trajectories in the quadrotor/joint space which will provide Quintic polynomial trajectories [29] as the

reference trajectories. By using these types of trajectories for the joint space control, we can avoid the vibrational modes because they have sinusoidal acceleration.

Parameters of DOb-based control is given in Table II. The controller is tested to stabilize and track the desired quadrotor/joint space trajectories under the effect of picking a payload of value $150g$ at instant $15s$ and placing it at instant $55s$. The simulation results in quadrotor/joint space are presented in Fig. 6. Fig. 7 shows response of system in the task space (the actual end-effector position and orientation can be found from the forward kinematics). These results show that the proposed motion control scheme able to track the desired trajectories, with achieving the control objectives. Figs. 8 shows the control effort, the required thrust forces and manipulator torques which are in the allowable limits.

V. CONCLUSION

The problem of the motion control of a new aerial manipulation robot called "Quadrotor Manipulation System" is presented. This robot has several issues in point of view the control system which have been addressed in this paper. Description and mathematical modeling of the proposed system are presented. Hybrid linear DOb/MPC based control design is proposed as a motion control system. The DOb
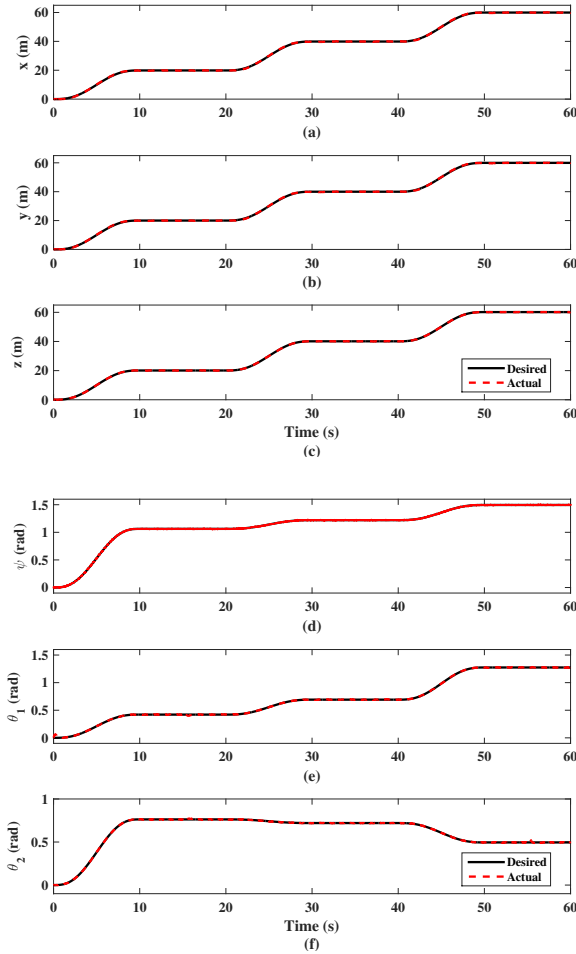
Fig. 6: The actual response of the Quadrotor/ Manipulator variables: a) x, b) y, c) z, d) ψ, e) θ_1, and f) θ_2

Fig. 7: The actual response of the end-effector position and orientation: a) x_e, b) y_e, c) z_e, d) ϕ_e, e) θ_e, and f) ψ_e

loop is used to enforce robust linear input/output behavior of the plant by canceling disturbances, measurement noise, and plant/model mismatch. After that the MPC controller is used in the external loop to achieve the required closed loop performance and control objectives with low computational load. The stability grandee is proved for this controller. The controller is tested to achieve trajectory tracking under the effect of picking/placing a payload, changing the operating region, and the measurement noise. The system is simulated using MATLAB/SIMULINK based on real parameters. Simulation results indicate the efficiency of the proposed controller.

ACKNOWLEDGMENT

REFERENCES

[1] S. Gupte, P. I. T. Mohandas, and J. M. Conrad, "A survey of quadrotor unmanned aerial vehicles," in *Southeastcon, 2012 Proceedings of IEEE*. IEEE, 2012, pp. 1–6.
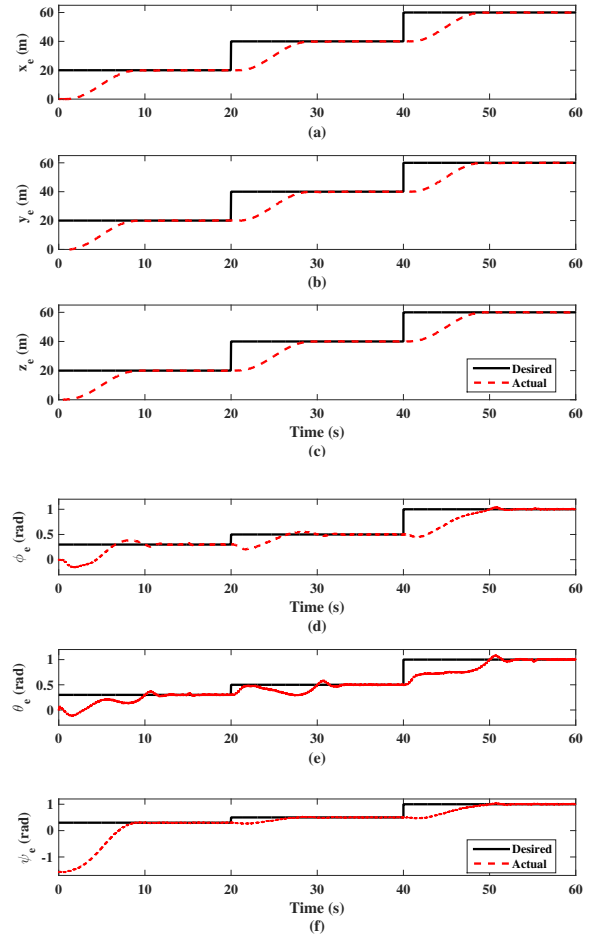
[2] S. Kim, S. Choi, and H. J. Kim, "Aerial manipulation using a quadrotor with a two dof robotic arm," in *Intelligent Robots and Systems (IROS), 2013 IEEE/RSJ International Conference on*. IEEE, 2013, pp. 4990–4995.

[3] D. Mellinger, Q. Lindsey, M. Shomin, and V. Kumar, "Design, modeling, estimation and control for aerial grasping and manipulation," in *2011 IEEE/RSJ International Conference on Intelligent Robots and Systems (IROS)*. IEEE, 2011, pp. 2668–2673.

[4] N. Michael, J. Fink, and V. Kumar, "Cooperative manipulation and transportation with aerial robots," *Autonomous Robots*, vol. 30, no. 1, pp. 73–86, 2011.

[5] A. Albers, S. Trautmann, T. Howard, T. A. Nguyen, M. Frietsch, and C. Sauter, "Semi-autonomous flying robot for physical interaction with environment," in *Robotics Automation and Mechatronics (RAM), 2010 IEEE Conference on*. IEEE, 2010, pp. 441–446.

[6] C. M. Korpela, T. W. Danko, and P. Y. Oh, "Mm-uav: Mobile manipulating unmanned aerial vehicle," *Journal of Intelligent & Robotic Systems*, vol. 65, no. 1-4, pp. 93–101, 2012.

[7] G. Heredia, A. Jimenez-Cano, I. Sanchez, D. Llorente, V. Vega, J. Braga, J. Acosta, and A. Ollero, "Control of a multirotor outdoor aerial manipulator," in *Intelligent Robots and Systems (IROS 2014), 2014 IEEE/RSJ International Conference on*. IEEE, 2014, pp. 3417–3422.

[8] F. Caccavale, P. Chiacchio, A. Marino, and L. Villani, "Six-dof impedance control of dual-arm cooperative manipulators," *Mechatronics, IEEE/ASME Transactions on*, vol. 13, no. 5, pp. 576–586, 2008.

[9] V. Lipiello and F. Ruggiero, "Cartesian impedance control of a uav with a robotic arm," in *10th IFAC Symposium on Robot Control*, 2012.
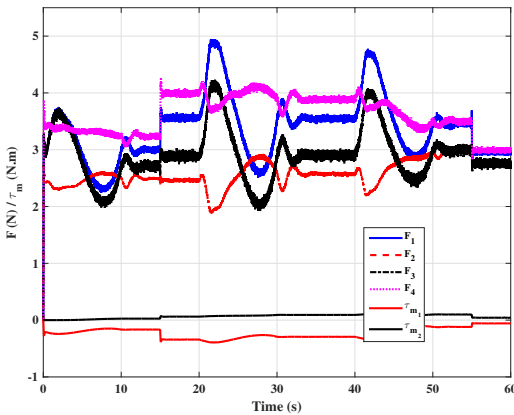
Fig. 8: The required controller efforts

[10] A. Khalifa, M. Fanni, A. Ramadan, and A. Abo-Ismail, "Modeling and control of a new quadrotor manipulation system," in *2012 IEEE/RAS International Conference on Innovative Engineering Systems*. IEEE, 2012, pp. 109–114.

[11] ——, "Adaptive intelligent controller design for a new quadrotor manipulation system," in *Systems, Man, and Cybernetics (SMC), 2013 IEEE International Conference on*. IEEE, 2013, pp. 1666–1671.

[12] M. Achtelik, M. Achtelik, S. Weiss, and R. Siegwart, "Onboard imu and monocular vision based control for mavs in unknown in-and outdoor environments," in *Robotics and automation (ICRA), 2011 IEEE international conference on*. IEEE, 2011, pp. 3056–3063.

[13] B. K. Kim and W. K. Chung, "Performance tuning of robust motion controllers for high-accuracy positioning systems," *Mechatronics, IEEE/ASME Transactions on*, vol. 7, no. 4, pp. 500–514, 2002.

[14] S. Li, J. Yang, W.-h. Chen, and X. Chen, *Disturbance observer-based control: methods and applications*. CRC Press, 2014.

[15] E. Sariyildiz, H. Yu, K. Yu, and K. Ohnishi, "A nonlinear stability analysis for the robust position control problem of robot manipulators via disturbance observer," in *Mechatronics (ICM), 2015 IEEE International Conference on*. IEEE, 2015, pp. 28–33.

[16] K. S. Eom, I. H. Suh, and W. K. Chung, "Disturbance observer based path tracking control of robot manipulator considering torque saturation," *Mechatronics*, vol. 11, no. 3, pp. 325–343, 2001.

[17] H.-T. Choi, S. Kim, J. Choi, Y. Lee, T.-J. Kim, and J.-W. Lee, "A simplified model based disturbance rejection control for highly accurate positioning of an underwater robot," in *Oceans-St. John's, 2014*. IEEE, 2014, pp. 1–5.

[18] T. Hsia, T. Lasky, and Z. Guo, "Robust independent robot joint control: design and experimentation," in *Robotics and Automation, 1988. Proceedings., 1988 IEEE International Conference on*. IEEE, 1988, pp. 1329–1334.

[19] E. Sariyildiz and K. Ohnishi, "A guide to design disturbance observer based motion control systems," in *Power Electronics Conference (IPEC-Hiroshima 2014-ECCE-ASIA), 2014 International*. IEEE, 2014, pp. 2483–2488.

[20] ——, "Stability and robustness of disturbance-observer-based motion control systems," *Industrial Electronics, IEEE Transactions on*, vol. 62, no. 1, pp. 414–422, 2015.

[21] J. B. Froisy, "Model predictive control: Past, present and future," *ISA transactions*, vol. 33, no. 3, pp. 235–243, 1994.

[22] D. Q. Mayne, J. B. Rawlings, C. V. Rao, and P. O. Scokaert, "Constrained model predictive control: Stability and optimality," *Automatica*, vol. 36, no. 6, pp. 789–814, 2000.

[23] L. Magni and R. Scattolini, "Model predictive control of continuous-time nonlinear systems with piecewise constant control," *Automatic Control, IEEE Transactions on*, vol. 49, no. 6, pp. 900–906, 2004.

[24] L. Wang, *Model predictive control system design and implementation using MATLAB®*. Springer Science & Business Media, 2009.

[25] T. Hatanaka, T. Yamada, M. Fujita, S. Morimoto, and M. Okamoto, "Nonlinear model predictive control towards new challenging applica-tions," *Nonlinear Model Predictive Control Towards New Challenging Applications*, vol. 384, pp. 561–569, 2009.

[26] G. Pin, D. M. Raimondo, L. Magni, and T. Parisini, "Robust model predictive control of nonlinear systems with bounded and state-dependent uncertainties," *Automatic Control, IEEE Transactions on*, vol. 54, no. 7, pp. 1681–1687, 2009.

[27] A. Ferrara, G. P. Incremona, and L. Magni, "A robust mpc/ism hierarchical multi-loop control scheme for robot manipulators," in *Decision and Control (CDC), 2013 IEEE 52nd Annual Conference on*. IEEE, 2013, pp. 3560–3565.

[28] C. Liu, W. Chen, and J. Andrews, "Trajectory tracking of small helicopters using explicit nonlinear mpc and dobc," in *18th IFAC World Congress, IFAC WC, Milano, Italy*, vol. 18, 2011, pp. 1498–1503.

[29] M. W. Spong, S. Hutchinson, and M. Vidyasagar, *Robot modeling and control*. Wiley New York, 2006, vol. 3.

[30] *Asctec Pelican Quadrotor*, Oct. 2014, available at http://www.asctec.de/en/uav-uas-drone-products/asctec-pelican/.

[31] L.-W. Tsai, *Robot analysis: the mechanics of serial and parallel manipulators*. Wiley-Interscience, 1999.

[32] P. J. From, J. T. Gravdahl, and K. Y. Pettersen, *Vehicle-Manipulator Systems*. Springer, 2014.

[33] T. Barry and L. Wang, "A model-free predictive controller with laguerre polynomials," in *Control Conference, 2004. 5th Asian*, vol. 1. IEEE, 2004, pp. 177–184.

[34] D. A. Wismer and R. Chattergy, *Introduction to nonlinear optimization: a problem solving approach*. North-Holland New York, 1978.

[35] B. D. Anderson and J. B. Moore, *Linear optimal control*. Prentice-hall Englewood Cliffs, 1971, vol. 197, no. 1.